Int. J. Cancer: **123,** 2684–2695 (2008)

Biophysical and biochemical characterization of a liposarcoma-derived recombinant MnSOD protein acting as an anticancer agent

Aldo Mancini[1]*, Antonella Borrelli[1], Antonella Schiattarella[1], Luigi Aloj[2], Michela Aurilio[2], Franco Morelli[3], Alessandra Pica[4], Antonella Occhiello[4], Roberto Lorizio[5], Roberto Mancini[5], Alessandro Sica[5], Lelio Mazzarella[6], Filomena Sica[6], Paolo Grieco[7], Ettore Novellino[7], Daniela Pagnozzi[8], Piero Pucci[8] and Jean Rommelaere[9]

[1]*Department of Molecular Biology and Biotherapy, National Cancer Institute "G. Pascale" Naples, Naples, Italy*
[2]*Department of Nuclear Medicine, National Cancer Institute "G. Pascale" Naples, Naples, Italy*
[3]*Institute of Genetic and Biophysic.-A. Buzzati Traverso Naples, Naples, Italy*
[4]*Department of Biological Science, University Federico II-Naples, Naples, Italy*
[5]*Department of Surgical Veterinary, University Federico II-Naples, Naples, Italy*
[6]*Department of Chemistry, University Federico II-Naples, Naples, Italy*
[7]*Department of Pharmacology and Toxicology, University Federico II-Naples, Naples, Italy*
[8]*Department of Organic Chemistry, University Federico II-Naples, Naples, Italy*
[9]*Deutsches Krebsforschungszentrum, Infection and Cancer Program, Abt.F010 and INSERM U701, Heidelberg, Germany*

A recombinant MnSOD (rMnSOD) synthesized by specific cDNA clones derived from a liposarcoma cell line was shown to have the same sequence as the wild-type MnSOD expressed in the human myeloid leukaemia cell line U937, except for the presence of the leader peptide at the N-terminus. These results were fully confirmed by the molecular mass of rMnSOD as evaluated by ES/MS analysis (26662.7 Da) and the nucleotide sequence of the MnSOD cDNA. The role of the leader peptide in rMnSOD was investigated using a fluorescent and/or ^{68}Gallium-labelled synthetic peptide. The labelled peptide permeated MCF-7 cells and uptake could be inhibited in the presence of an excess of oestrogen. *In vivo* it was taken up by the tumour, suggesting that the molecule can be used for both therapy and diagnosis. The *in vitro* and *in vivo* pharmacology tests confirmed that rMnSOD is only oncotoxic for tumour cells expressing oestrogen receptors. Pharmacokinetic studies in animals performed with ^{125}I- and ^{131}I-labelled proteins confirmed that, when administered systemically, rMnSOD selectively reached the tumour, where its presence was unambiguously demonstrated by scintigraphic and PET scans. PCR analysis revealed that *Bax* gene expression was increased and the *Bcl2* gene was down regulated in MCF7 cells treated with rMnSOD, which suggests that the protein induces a pro-apoptotic mechanism.

Key words: rMnSOD; anticancer agent; free radicals; antioxidant

Chromosomal abnormalities have long been known to be involved in cancer development. However, only with the advances made in cytogenetics and molecular biology in the last 2 decades was the genetic basis of neoplasia firmly established and chromosomal alterations recognized as being critical in the pathogenesis of human cancer. Chromosomal changes frequently involve proto-oncogenes and their deregulation is associated with the development of malignancy.[1–3] Recurrent chromosomal alterations provide cytological and molecular markers for the diagnosis and prognosis of the disease. They also facilitate the identification of genes that are important in carcinogenesis and that may eventually lead to the development of a targeted drug therapy. Most of the genetic alterations found in cancer cells are caused by chromosomal translocations. When 2 or more chromosomes split and 1 or more fragments are exchanged among them, chromosomes are rearranged and the corresponding gene products (*i.e.,* fusion or hybrid proteins) can fulfil new functions or undergo loss of function, all in order to maintain the malignant phenotype.[4] In this sense it is likely that the molecular basis of tumours rests on proteins derived from chromosomal aberrations that give tumour cells selective clonal advantages in order to maintain the transformed phenotype and to escape homeostatic control. An example of these selective advantages is seen in the expression of proteins such as the metalloproteinases that are produced and released by tumour cells and are active in the degradation of basal membranes, and thus playing a crucial role in tumour metastasis and angiogenesis.[5] Cancer cells also provide themselves with environmental advantages such as new blood vessels to get a better supply of oxygen and nutrients.[6] One means by which tumours achieve this goal is through the activation of the oxidative stress system. It was shown that nitric oxide synthetase[7] and gp^{91}phox,[8] 2 free radical-generating enzymes, trigger vascular endothelial growth factor production and promote oncogenesis. The crucial role of proteins in maintaining the transformed phenotype, along with the striking interdependence of protein structure and protein functions in cancer cells, prompted us to investigate a liposarcoma cell line that produced and released a number of proteins used for autocrine growth in culture medium.[9] Among these, a novel isoform of manganese superoxide dismutase (LSA-type MnSOD) was recently identified.[10] In addition to the enzymatic activity common to all SODs directed to transform free radicals into hydrogen peroxide,[11–13] the LSA-type MnSOD showed peculiar structural and functional properties that are different from the corresponding native MnSOD molecule expressed in the human myeloid leukaemia cell line U937 (Swiss Prot. Code P04179).[14] The LSA-type MnSOD, in fact, is secreted by LSA cells whereas native MnSOD is located in the mitochondrial matrix.[15] The molecular weight of the LSA-type MnSOD is about 30 kDa, as estimated by SDS-PAGE,[10] which is significantly higher than the value of 24 kDa calculated for human native MnSOD.[16] Finally, and more importantly, when injected *in vitro* or *in vivo*, the LSA-type MnSOD permeates and selectively kills tumour cells, provided that they express oestrogen receptors and low levels of catalase. In contrast, normal cells are not affected by the protein, making the cytotoxic activity of LSA-type MnSOD specific for tumour cells.[10] Therefore, a recombinant form of LSA-type MnSOD (rMnSOD) was produced from specific cDNA clones and demonstrated to retain both the structural and oncotoxic properties of the native protein.[10] In this article we characterize the biophysical and biochemical properties of rMnSOD and report on its pharmacokinetic properties and biodistribution *in vivo*. A possible mechanism of action is also proposed. The detailed structural investigation clearly indicated that rMnSOD has the same sequence as the native protein. However, both the recombinant and the original LSA-type MnSOD form carry the 24-residue leader peptide at the N-terminus. These results were fully confirmed by the molecular mass of rMnSOD, as evaluated by mass spectrometry (26662.7 Da), and the nucleotide sequence of the corresponding cDNA. The role of the leader peptide was

***Correspondence to:** National Cancer Institute of Naples, Via Mariano Semmola 80131, Naples, Italy. Fax: 0039-081-5903720.
E-mail: aldo_mancini@tiscali.it
Received 20 November 2007; Accepted after revision 30 May 2008
DOI 10.1002/ijc.23791
Published online 16 September 2008 in Wiley InterScience (www.interscience.wiley.com).

investigated using a fluorescent and/or ^{68}Gallium-labelled synthetic peptide. The labelled peptide showed the same properties as the whole rMnSOD molecule. It could be specifically taken up by ER^+ MCF-7 cells or tumour cells in dogs with spontaneous mammary tumours. A radiolabelled version of rMnSOD showed a specific and selective ability to reach tumours expressing oestrogen receptors in tumour-bearing animals and to induce massive cytotoxic effects in the target cells. According to our data, these molecules might be suitable for use as anticancer agents, tumour markers for imaging analysis and even as radiopharmaceutical vehicles. Finally, PCR analyses indicated that *Bax* gene expression was induced and the *Bcl2* gene down regulated in treated MCF7 cells, suggesting a pro-apoptotic effect of rMnSOD.

Material and methods

Antibodies and reagents

Primary antibodies. MnSOD-specific sheep polyclonal anti-serum raised against highly purified MnSOD from human liver does not cross-react with Cu/ZnSOD in double-diffusion tests (Calbiochem #574596, Germany).

Secondary antibodies. As secondary antibodies, 15-nm colloidal gold-coupled donkey anti-sheep IgGs (Aurion, The Netherlands) and horseradish peroxidase-coupled rabbit anti-sheep IgGs (Promega, Germany) were used.

Immunoaffinity purification of E. coli *recombinant rMnSOD*

Bacteria were washed in PBS and lysed in buffer A (4.29 mM Na_2HPO_4, 1.47 mM KH_2PO_4, 2.7mM KCl, 137 mM NaCl, 0.5mM PMSF, pH 7.3) using a cell disrupter (Constant Systems Ltd, Mode code 01/40/AA). The supernatant (extract) was collected after centrifugation of the lysates for 15 min at 13,200 r.p.m. in an Eppendorf F452411 rotor at 4°C. The extract was loaded onto a T7 tag antibody agarose resin (Novagen), equilibrated and washed in buffer A. This was then eluted with 100 mM citric acid, pH 2.2. The collected fractions were neutralized with 2 M Tris base, pH 10.4, and aliquots were analyzed by 12% polyacrylamide SDS-PAGE.

Characterization of full-length rMnSOD

Native and chemically modified rMnSOD were desalted by using HP 1100 HPLC (Agilent Technologies) with a C_4 narrow-bore reverse-phase column (Phenomenex 250 × 2.00 mm^2) at a flow rate of 200 μL/min. Mobile phase was 0.1% trifluoroacetic acid (eluent A) and 95% acetonitrile, 0.07% trifluoroacetic acid (eluent B). Protein samples were reduced with a 10-fold molar excess of DTT over all SH groups by incubation for 2 hr at 37°C in 6 M Guanidinium/HCl, 250 mM Tris/HCl, 1.2 mM EDTA buffer, pH 8.5. Carboxyamidomethylation of cysteine residues was performed by applying a 10-fold molar excess of iodoacetamide over all the SH groups for 30 min at room temperature in the dark. The molecular mass of native, reduced and carboxyamidomethylated rMnSOD was determined by electrospray mass spectrometry (ESMS) on a Quattro-Micro triple quadrupole mass spectrometer (Waters-Micromass). Protein solution was injected into the ion source at a flow rate of 10 μL/min. Data were processed using the Mass Lynx program (Waters-Micromass). The N-terminal amino acid sequence of rMnSOD was obtained by Edman degradation on an automated Procise H49 sequencer (Applied Biosystems).

Peptide mapping of rMnSOD

Aliquots of rMnSOD were individually hydrolyzed by incubation with different proteases (trypsin, endoprotease Lys-C, and endoprotease V8) at 37°C overnight in 50-mM NH_4HCO_3 buffer, pH 8.0, using a 1/50 (w/w) enzyme to substrate ratio. The resulting peptide mixtures were directly analyzed by MALDI mass spectrometry. MALDI mass spectra were recorded on a Voyager DE-PRO mass spectrometer equipped with a reflectron analyzer operating in delayed extraction mode (Applied Biosystem). An amount of 1 μL of peptide sample was mixed with an equal volume of α-cyano-4-hydroxycynnamic acid as matrix [in acetonitrile/50-mM citric acid (70:30, v/v)], applied to the metallic sample plate, and air dried. Mass calibration was performed by using the standard mixture provided by the manufacturer. Peptides obtained from endoprotease V8 digestion were also fractionated by HPLC, using a C_{18} narrow-bore reverse-phase column (Phenomenex 250 × 2.00 mm^2) at a flow rate of 200 μL/min. Collected fractions were directly analysed by MALDI mass spectrometry and selected samples were sequenced by Edman degradation.

Characterization of LSA-type MnSOD

Start material (LSA-CM) was prepared as previously described[10] and then concentrated 12-fold by ultrafiltration through Amicon filters to a cut-off point of 3,000 Da. Proteins were fractioned by discontinuous 12% SDS-PAGE and blotted onto nitrocellulose membranes according to Ref. 17. The protein of interest (LSA-type MnSOD) was incubated in a 1:300 dilution of anti-MnSOD anti-serum in 10% dry milk/PBS and stained using horseradish peroxidase-conjugated donkey anti-sheep IgG and then detected by ECL (Perkin-Elmer, Germany).

LSA-type MnSOD protein band was excised from the gel and destained by repeated washings with 50-mM NH_4HCO_3, pH 8.0 and acetonitrile. The sample was reduced and carboxyamidomethylated with 10-mM DTT and 55-mM iodoacetamide in 50-mM NH_4HCO_3 buffer, pH 8. The alkylated sample was digested at 37°C overnight using 100 ng of trypsin. The peptide mixture was fractionated by LCMSMS analysis, performed on a Q-TOF hybrid mass spectrometer equipped with a Z-spray source and coupled on-line with a capillary chromatography system CapLC (Waters, Manchester, UK). After loading, the peptide mixture (6 μL) was first concentrated and washed at 10 μL/min onto a reverse-phase pre-column using 0.2% formic acid as eluent. The sample was then fractionated onto a C_{18} reverse-phase capillary column (75 μm × 20 mm) at a flow rate of 250 nL/min using a linear gradient of eluent B (0.2% formic acid in 95% acetonitrile) in A (0.2% formic acid in 5% acetonitrile) from 7 to 60% in 50 min. The mass spectrometer was set up in a data-dependent MS/MS mode where a full-scan spectrum (*m/z* acquisition range from 400 to 1,600 Da/e) was acquired and then a tandem mass spectrum (*m/z* acquisition range from 100 to 2,000 Da/e). Peptide ions were selected as the 3 most intense peaks of the previous scan. Suitable collision energy was applied, depending on the mass and charge of the precursor ion. ProteinLynx software, provided by the manufacturers, was used to analyze raw MS and MS/MS spectra and to generate a peak list, which was introduced into the Mascot MS/MS ion search software for protein identification.

Determination of rMnSOD nucleotide sequence

To verify the identity of the rMnSOD, we sequenced the entire coding region of the gene cloned in the pET $21A^+$ plasmid. To sequence the cDNA inserted in the Eco R1 restriction site of the polylinker, we used the T7 promoter and T7 terminator primers localized at the 5′ and 3′ of the vector's multiple cloning site, respectively. Moreover, we used, for the sequence analysis, an internal primer (SOD500/AGCTGACGGCTGCCATCTGTT) located 269 bases upstream of the stop codon to confirm the exact nucleotide sequence encoding to the protein C-terminus.

Determination of MnSOD enzymatic activity and hydrogen peroxide concentration in rMnSOD-treated target cells

To measure MnSOD activity in target cells, exponentially growing MCF-7 and MRC-5 cultures (2×10^7 cells) were treated or not treated with 1.5-μM rMnSOD for 24 hr and the MnSOD activity assayed using a commercially available SOD assay kit (Calbiochem, Darmstadt, Germany) according to the manufacturer's instructions. Commercially available recombinant SOD (Sigma-Aldrich, Germany) and concentrated LSA-CM were used as con-

trols. Hydrogen peroxide concentrations were measured in 3×10^5 cells from similarly treated cultures, using a commercially available kit (TEMA, Bologna, Italy) according to the manufacturer's recommendations. This kit is based on a biochemical colorimetric reaction of xylenol orange in an acid environment containing sorbitol and ammonium iron sulphate. Upon addition or production of hydrogen peroxide the intensity of the colour changes proportional to the H_2O_2 concentration.

Circular dicroism

Circular dicroism (CD) spectra were recorded with a Jasco J-715 spectropolarimeter equipped with a Peltier-type temperature control system (model PTC-348WI). CD was calibrated using (1S)-(+)-10-camphorsulphonic acid (Aldrich, Milwaukee, WI), which exhibits a 34.5 M/cm molar extinction coefficient at 285 nm and 2.36 M/cm molar ellipticity at 295 nm. Before the measurements, the sample was equilibrated at the desired temperature for 5 min. The molar ellipticity per mean residue, $[\lambda]$ (deg cm^2 dmol^{-1}), was calculated according to the equation $[\lambda] = [\lambda]_{obs}(mrw)/10lC$, where $[\lambda]_{obs}$ is the ellipticity (deg), mrw is the mean residue molecular weight, 111 Da, C is the protein concentration (g mL^{-1}) and l is the optical path length of the cell (cm). A 0.1-cm path length cell and a protein concentration of about 0.05 mg mL^{-1} in 20-mM ammonium trifluoracetate, pH 7.8, were used. CD spectra were recorded with a time constant of 4 s, a 2-nm bandwidth and a scan rate of 5 nm min^{-1}. Four spectra were averaged after baseline correction by subtracting a buffer spectrum. The percentages of secondary structures were calculated by using online CD analysis, DICHROWEB (http://www.cryst.bbk.ac.uk/cdweb/html/), which provides several algorithms to analyze the curves. CD data were analyzed by 3 different programs: CDSSTR, which implements the variable selection method by performing all possible calculations with a fixed number of proteins from a reference set; SELCON3, which incorporates a self-consistent method together with the singular value decomposition algorithm (SVDA) to assign protein secondary structure; and CONTIN/LL, which implements the ridge regression algorithm of Provencher and Glockner, incorporating the locally linearized model of Van Stokkum. Far-UV CD at 222 nm was used to monitor thermal unfolding of the protein. The temperature was raised from 15 to 110°C at a rate of 0.5°C/min. At the end of each experiment, the sample was cooled immediately to room temperature and spectra were recorded to monitor the extent of re-folding. The denaturing temperature (T_m) was estimated to be 59 ± 2°C from the first derivative of the CD data as a function of temperature. Protein solution was analyzed for total metal content by flame atomic absorption spectrometry. Manganese concentration was determined by comparison with a calibration curve. A Varian SpectrAA 220 atomic absorption spectrometer equipped with an MK7 burner was used for the analyses.

Immunocytochemistry: Light microscopy

Tumour cells were fixed in Zamboni solution (4% paraformaldehyde, 15% picric acid) for 15 min, washed with PBS and blocked for an additional 15 min in PBS containing 1% bovine serum albumin (BSA) and 0.15% glycine. For immunodetection the cells were incubated with a 1:20 dilution of sheep anti-MnSOD anti-serum at 4°C overnight, followed by further incubation with 10 nm colloidal gold-coupled donkey anti-sheep IgGs for 2 hr at room temperature. By treating the samples with silver enhancer for 6 min (Sigma-Aldrich, Germany), antibody complexes were revealed, which were then rinsed in sodium thiosulphate and distilled water and counterstained with Mayer's haemalum solution. These samples were examined using the Kontron Electronic Imaging Computer System KS300. Imaging was performed using a Kontron Electronic Progress 3008 camera.[18]

Inhibition of rMnSOD uptake in MCF-7 cells by estradiol: immunocytochemical determination

MCF-7 cells were seeded in 2 different chamber slides containing 16 well/chamber (NUNC) in DMEM supplemented with 10% FCS at a density of 5,000 cells/well and incubated at 37°C. After 24 hr, the test cells were treated with a 1.5-μM rMnSOD and a cold 10-nM estradiol solution in DMEM supplemented with 10% FCS. Control cells were treated with DMEM + 10% FCS + 1.5-μM rMnSOD and DMEM + 10% FCS, respectively. Experiments were performed in triplicate.

Radiolabelling and biodistribution of rMnSOD

rMnSOD was labelled with ^{125}I or ^{131}I, using IODO-GEN precoated iodination tubes (Pierce, Rockford, IL) according to the manufacturer's suggested procedure. Briefly, 200 μg of protein were added to the iodination tubes in a 200-μL volume of phosphate-buffered saline. To the protein solution we added 500 μCi of Na-^{125}I (Amersham Biosciences UK Limited, Buckinghamshire, UK) and incubated this for 15 min. Labelled protein was recovered by gel filtration on D-salt polyacrylamide columns (Pierce). Label incorporation was 90%. Biodistribution was measured in a tumour-bearing dog as described in the legend to Figure 4.

Synthesis of rMnSOD leader peptide in solid phase

The 24-residue leader peptide MLSRAVCGTSRQLAPALGYLGSRQ sequence and a scrambled peptide sequence QSRMLSCTGRAVLRGLGYLLASQPAGG were synthesized using the solid-phase approach and standard Fmoc methods in a manual reaction vessel. The samples were purified by semi-preparative RP-HPLC using C18-bonded silica column (Vydac 218TP1010). The purified peptide was 99% pure as determined by analytical RP-HPLC. The correct molecular mass of the peptide was confirmed by mass spectrometry and amino acid analysis.[19]

Confocal analysis

MCF7-cells cultivated in glass bottom polystyrene dishes were incubated with 1.5-μM FITC-labelled peptide for 1 hr at room temperature, washed with PBS, incubated in 2% paraformaldehyde-PBS for 1 hr at room temperature, and washed with PBS. The labelled cells were analyzed using a Zeiss LSM 510 confocal laser scanning microscope. Control cells were treated first with 1-μM oestrogen and then processed in the same manner as the treated cells. Fluorescent images were analyzed with the Meta Morph Imaging System software (Universal Imaging Corporation, West Chester, PA).

Radioisotopes

^{131}I was purchased from Amersham and ^{68}Gallium was synthesized by the Department of Nuclear Medicine of the National Cancer Institute (Naples, Italy).

Radiolabelling with ^{68}Ga-labelled DOTA-coupled leader peptide and PET imaging

Approximately 20 μg of DOTA-coupled MLSRAVCGTSRQ LAPALGYLGSRQ peptide, corresponding to the leader sequence of rMnSOD, were labelled with ^{68}Ga at 120°C for 15 min in Hepes buffer. The labelled peptide was purified by passing it through a C18 reversed-phase cartridge which was washed with water and subsequently air dried. The peptide was recovered with ~400 μL of 96% ethanol. Then, 1 mCi of the labelled peptide was injected intravenously into the front-limb of a 13-year-old female mongrel dog weighing 15 kg that had been referred by the Department of Medicine and Surgery, Faculty of Veterinary Medicine, University of Naples, Federico II. The animal was affected by spontaneous multiple breast cancer lesions. Informed consent was obtained from the dog's owner prior to performing the PET studies and rMnSOD treatments. Images were acquired ~30 min after injection on a Siemens ECAT 47 PET scanner. Images were reconstructed in the transaxial, coronal and sagittal planes.

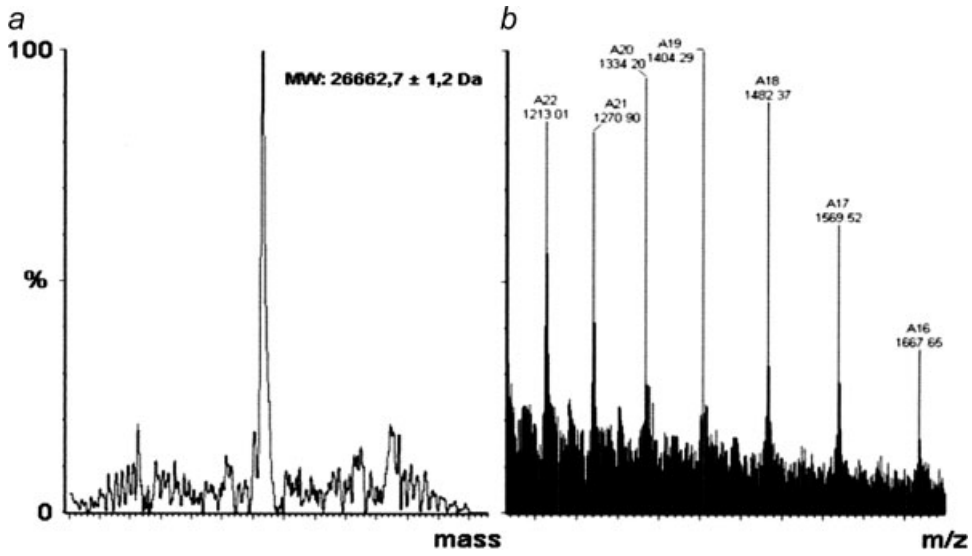

Figure 1 – Structural analysis of rMnSOD. Electrospray mass spectrometry (ESMS) analysis of recombinant rMnSOD showing the accurate molecular mass of 26662.7 ± 1.2Da (*a*). MALDI/MS analysis of the rMnSOD endoprotease V8 digestion products. Assignment of mass signals to individual peptides within the protein sequence is indicated (*b*).

PCR analyses

Three samples of MCF7 breast cancer cells were cultured for 4 hr in DMEM 10% FCS containing 1.5-μM rMnSOD. Three control samples consisting of MCF-7 cells in the absence of rMnSOD were maintained in identical culture conditions. Total RNA was extracted from MCF-7 cells cultured in the presence or in the absence of rMnSOD (Chomczynski and Sacchi procedure, RNAzol, Invitrogen) according to the manufacturer's instructions, and its integrity was verified by agarose gel electrophoresis.

From each of the 6 samples 2 μg of total RNA in a final volume of 20 μL was reverse-transcribed by Avian myeloblastosis virus (AMV) reverse transcriptase (Gibco BRL Invitrogen) according to the manufacturer's instructions at 37°C for 60 min using random hexamer primers. PCR analysis of both *Bax* and *Bcl2* gene expression was performed by using a Gene Amp PCR system 9700 (Applied Biosystem) and hot start Taq Gold (Applera). Actin was used as a housekeeping control gene. The following primers were used: *Bax* Fw CCA GCT CTG AGC AGA TCA TG; *Bax* Rw AAG ATC CTG GCA GAG AGG AG; *Bcl2* Fw GAC TTC GCC GAG ATG TCC AG; *Bcl2* Rw CAG GTG CCG GTT CAG GTA CT; Actin Fw GAC TAC CTC ATG AAG ATC CT; and Actin Rw GCT TGC TGA TCC ACA TCT GC. PCR conditions were: initial denaturation at 95° for 10 min followed by 35 cycles: 95°, 45′′; 54° , 45′′ and 72° 45′′ with a final extension at 72° for 10 min. The amplification products were fractionated on a 1% agarose gel in 0.5 × TBE (Tris Borate EDTA) buffer to control the amplicon lengths.

Results

Immunoaffinity purification of rMnSOD

Human T7-tagged rMnSOD was purified from *E.coli* cell extract through a single immunoaffinity chromatography step on a T7 tag antibody agarose column equilibrated and washed in phosphate buffer. The retained proteins were eluted by lowering the pH to 2.2 with 100-mM citric acid. Collected fractions were neutralized with 2-M Tris base, pH 10.4, and aliquots were analyzed by SDS-PAGE to verify the purity grade. Fractions containing a single protein band were pooled and structurally characterized in detail.

Characterization of full-length rMnSOD

Purified native and carboxyamidomethylated rMnSOD samples were first analyzed by ESMS. The native protein exhibited a molecular mass of 26662.7 ± 1.2 Da (Fig. 1*a*). This mass value increased to 26895.6 ± 0.9 Da following alkylation of the protein with iodoacetamide, with a mass difference of 232.8 Da corresponding to four carboxyamidomethyl groups that were incorporated, and hence revealing the occurrence of four cysteine residues. The N-terminal sequence of the first 20 amino acids of rMnSOD, as determined by automated Edman degradation, confirmed the presence of the entire T7 tag (15 amino acids) at the N-terminus of the protein. The other 5 residues corresponded to the leader peptide of human MnSOD, indicating that the purified protein had not been proteolytically processed. The human MnSOD sequence reported in the Swiss Prot database (code: P04179) encompasses 221 residues (without the N-terminal Met), including a 24-residue leader peptide for mitochondrial import, and contains 3 Cys residues. This sequence accounts for a molecular mass of 24722.1 Da. When including the 15-residue peptide tag, the theoretical mass value for rMnSOD (236 residues) increases to 26247.6 Da.

Peptide mapping of rMnSOD and LSA-type MnSOD

Peptide mapping of rMnSOD was carried out using 3 different proteases (trypsin, endoprotease Lys-C and endoprotease V8). Aliquots of the reduced and carboxyamidomethylated recombinant protein were individually digested with the 3 enzymes and the resulting peptide mixtures directly analyzed by MALDI mass spectrometry. Mass signals recorded in the spectra were assigned to individual peptides within the rMnSOD sequence according to their molecular mass and the specificity of the proteases (Fig. 1*b*). The MALDI mass spectra demonstrated an almost complete coverage of the protein sequence from the N-terminal amino acid to residue 236. However, as stated above, the protein sequence confirmed by the mass mapping procedure did not account for the experimental mass value determined by ESMS. Taken together, these data suggest that the peptide extension might have been located at the C-terminus. Moreover, 2 mass signals at *m*/*z* 1431.6 and 1874.9 in the MALDI spectra that were obtained after endoprotease V8 digestion could not be assigned to any peptide within the rMnSOD sequence, suggesting that these fragments might

TABLE I – DETERMINATION OF THE NUCLEOTIDIC SEQUENCE OF RECOMBINANT rMnSOD cDNA

acgcgggactcgtggctgtggtggcttcggcagcggcttcagcagatcggcggcatcagcggtagcaccagcactagcagc																			
ATG	TTG	AGC	CGG	GCA	GTG	TGC	GGC	ACC	AGC	AGG	CAG	CTG	GCT	CCG	GCT	TTG	GGG	TAT	CTG
M	L	S	R	A	V	C	G	T	S	R	G	S	A	P	A	L	G	Y	L
GGC	TCC	AGG	CAG	AAG	CAC	AGC	CTC	CCC	GAC	CTG	CCC	TAC	GAC	TAC	GGC	GCC	CTG	GAA	CCT
G	S	R	Q	K	H	S	L	P	D	L	P	Y	D	Y	G	A	L	E	P
CAC	ATC	AAC	GCG	CAG	ATC	ATG	CAG	CTG	CAC	CAC	AGC	AAG	CAC	CAC	GCG	GCC	TAC	GTG	AAC
H	I	N	A	Q	I	M	Q	L	H	H	S	K	H	H	A	A	Y	V	N
AAC	CTG	AAC	GTC	ACC	GAG	GAG	AAG	TAC	CAG	GAG	GCG	TTG	GCG	AAG	GGA	GAT	GTT	ACA	GCC
N	L	N	V	T	E	E	K	Y	Q	E	A	L	A	K	G	D	V	T	A
CAG	ATA	GCT	CTT	CAG	CCT	GCA	CTG	AAG	TTC	AAT	GGT	GGT	GGT	CAT	ATC	AAT	CAT	AGC	ATT
Q	ILE	A	L	Q	P	A	L	K	F	N	G	G	G	H	I	N	H	S	I
TTC	TGG	ACA	AAC	CTC	AGC	CCT	AAC	GGT	GGT	GGA	GAA	CCC	AAA	GGG	GAG	TTG	CTG	GAA	GCC
F	W	T	N	L	S	P	N	G	G	G	E	P	K	G	E	L	L	E	A
ATC	AAA	CGT	GAC	TTT	GGT	TCC	TTT	GAC	AAG	TTT	AAG	GAG	AAG	CTG	ACG	GCT	GCA	TCT	GTT
I	K	R	D	F	G	S	F	D	K	F	K	E	K	L	T	A	A	S	V
GGT	GTC	CAA	GGC	TCA	GGT	TGG	GGT	TGG	CTT	GGT	TTC	AAT	AAG	GAA	CGG	GGA	CAC	TTA	CAA
G	V	Q	G	S	G	W	G	W	L	G	F	N	K	E	R	G	H	L	Q
ATT	GCT	GCT	TGT	CCA	AAT	CAG	GAT	CCA	CTG	CAA	GGA	ACA	ACA	GGC	CTT	ATT	CCA	CTG	CTG
I	A	A	C	P	N	Q	D	P	L	Q	G	T	T	G	L	I	P	L	L
GGG	ATT	GAT	GTG	TGG	GAG	CAC	GCT	TAC	TAC	CTT	CAG	TAT	AAA	AAT	GTC	AGG	CCT	GAT	TAT
G	I	D	V	W	E	H	A	Y	Y	L	Q	Y	K	N	V	R	P	D	Y
CTA	AAA	GCT	ATT	TGG	AAT	GTA	ATC	AAC	TGG	GAG	AAT	GTA	ACT	GAA	AGA	TAC	ATG	GCT	TGC
L	K	A	I	W	N	V	I	N	W	E	N	V	T	E	R	Y	M	A	C
AAA	AAT	AAG	AAT	TCA	TGT														
K	N	K	N	S	C														

Nucleotide sequence of the rMnSOD cDNA inserted in the Eco R1 restriction site of the polylinker.

very likely contain the additional amino acid residues. The endoprotease V8 digestion product was then fractionated by HPLC and the individual fractions were manually collected and directly analyzed by MALDI mass spectrometry. The fraction containing the peptide with a mass value of 1431.6 Da was identified and submitted to automated Edman degradation and demonstrated the following amino acid sequence: ArgTyrMetAlaCysLysAsnLysAsnSerCys. This sequence indeed corresponded to the C-terminal peptide of rMnSOD from 231 to 236 plus the additional 5-residue sequence Asn-Lys-Asn-Ser-Cys. This extension contained the fourth cysteine residue predicted previously by ESMS analysis. Moreover, the calculated molecular mass of the rMnSOD including the C-terminal extension (26666.2 Da) was in perfect agreement with the experimental value determined by ESMS.

Once the recombinant form of MnSOD was characterized, the structural analysis was also extended to the LSA-type MnSOD, the isoform secreted by LSA cells and endowed with anti-tumoural activity.[10] The LSA-secreted proteins were fractionated by SDS-PAGE and the protein band likely corresponding to the MnSOD was excised from the gel, digested *in situ* with trypsin and identified by using LC-MS/MS methods.[20] Once the exact electrophoretic mobility of LSA-type MnSOD was established, a peptide map of the secreted protein was constructed by tryptic digestion of the corresponding gel band. The resulting peptide mixture was directly analyzed by MALDI mass spectrometry and the mass signals recorded in the spectra were assigned to individual peptides within the rMnSOD sequence according to their molecular mass and the specificity of the proteases as described above for rMnSOD. Peptide mapping of the LSA-type MnSOD essentially confirmed the presence of the leader peptide at the N-terminus of the protein. In fact, the mass signals at m/z 2464.6 and 2333.4 corresponded to the N-terminal peptide of the MnSOD precursor form with and without the initial Met residue. As expected, the C-terminal end of the LSA secreted protein did not show the additional 5-amino acid peptide, as indicated by the mass signal at *m*/*z* 816.5 corresponding to the oxidized form of the C-terminal peptide 217-222.

Sequence analysis of rMnSOD

The entire coding region of the gene for rMnSOD was verified by cDNA sequencing. The T7 promoter and T7 terminator primers localized at 5′ and 3′ of the vector's multiple cloning site were used to sequence the cDNA inserted in the Eco R1 restriction site of the polylinker (Table I). Moreover, an internal primer located at position 500 of the coding sequence was used to confirm the exact nucleotide sequence corresponding to the 5 additional amino acids at the protein's C-terminus (Table I). The data obtained from the fine sequence analysis clearly demonstrated that a single point mutation had occurred after the codon corresponding to Lys 221 of the protein sequence, generating a new stretch of 5 codons: AAT AAG AAT TCA TGT corresponding to the amino acids N K N S C. The addition of these amino acids was due to the loss of a G in position 666 in the cDNA sequence either during cloning or amplification of the rMnSOD cDNA. The loss of this base generated a frame shift in which the last Lys codon normally present in the human MnSOD sequence was modified and the terminator codon TAA lost. Translation proceeded using the nucleotides of the vector and this shift produced the additional 5 amino acids (Table I).

CD

Figure 2*a* shows the CD spectrum of the protein characterized by a strong positive band at 192 nm and 2 strong negative bands at 210 and 222 nm. Quantification of the overall secondary structure of rMnSOD (see *Material and methods*) indicates 50% of α-helix, 15% of β-sheet and 15% of turns. The results are in line with those determined from the X-ray structure of human MnSOD.[21] The change in ellipticity of rMnSOD at 222 nm with temperature is plotted in Figure 2*b*, which indicates an apparent T_m value of 59°C, taken as the midpoint of the unfolding transition. Therefore, this protein is less stable than the human native enzyme. For the latter, differential scanning calorimetry[22] showed the first inactivation step at 68°C, followed by a main unfolding transition at about 88°C. Metal analysis, performed by atomic absorption spectroscopy, revealed that about two thirds of the metal binding sites are occupied by manganese ions.

MnSOD enzymatic activity and hydrogen peroxide concentration in rMnSOD-treated cells

Intracellular MnSOD activity and hydrogen peroxide production were both measured in susceptible MCF-7 and resistant MRC-5 cells prior to and after rMnSOD treatment. Although resulting in a modest increase in the overall MnSOD activity of MCF-7 cells (900 ± 8 U/mg to 1,250 ± 8 U/mg protein), exoge-

nously applied rMnSOD enhanced the hydroxide peroxide levels in MCF-7 cultures dramatically, as detected in both cell pellets and medium supernatants. In fact, the H_2O_2 concentration in MCF-7 cultures increased from basal levels of 38.3 ± 1.8 (cell-associated) and 0.0 ng/mL (medium) to 322.9 ± 2.8 and 690 ± 5.4 ng/mL, respectively, after rMnSOD treatment. In contrast, the cell-associated H_2O_2 concentrations in resistant MRC-5 cells remained constant at about 30 ng/mL, regardless of whether cultures had been treated with rMnSOD or not.

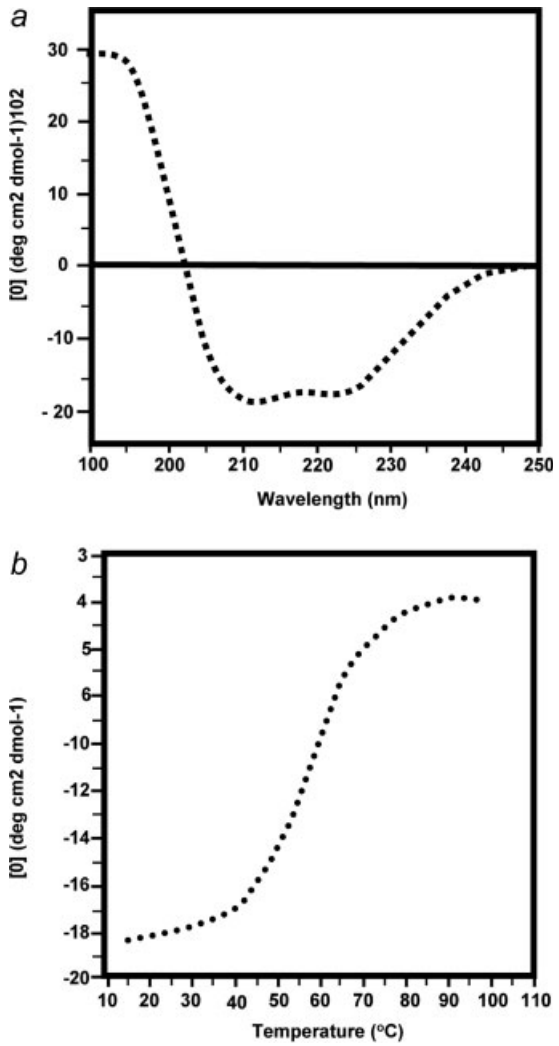

Figure 2 – Circular dicroism analysis of rMnSOD. (*a*) CD spectrum of rMnSOD in 20-mM ammonium trifluoracetate, pH 7.8, at 10 °C. (*b*) Thermal transition curve obtained by recording the molar ellipticity at 222 nm.

In vivo *pharmacology*

The pharmacological effect of rMnSOD on *in vivo* tumour growth was investigated using 60 nude mice bearing A2780 cell xenografts derived from a human ovarian adenocarcinoma. Two groups consisting of 6 animals each were used as controls. The first group remained untreated whereas the other received only PBS by injection. When the size of the tumour mass reached 1.5 cm, the animals were injected intraperitoneally (i.p.) with increasing daily doses of rMnSOD and tumour growth evaluated (Table II). From this experiment we could establish the amount of rMnSOD needed to completely inhibit tumour growth. All these observations were made over a period of 15 days. The experiments were stopped at Day 15 because the tumours in the animals of the control groups grew rapidly, limiting their ability to move, eat and drink.

Biodistribution of ^{125}I-labelled rMnSOD after injection into normal and tumour-bearing animals

For biodistribution studies, normal animals or animals bearing A2780 cell xenografts derived from a human ovarian adenocarcinoma were injected i.p. with 4 μg of labelled protein (Fig. 3). The animals were killed 3 hr after injection, dissected and organs counted in a single-well gamma counter. Dilutions of the injected compound were also counted to accurately determine the injected dose. The relative amount of radioactivity in the organs was calculated and expressed as a percentage of the injected dose/gram tissue (%ID/g).

Localization of ^{131}I-rMnSOD in a dog with breast cancer

In vivo localization of rMnSOD was monitored by treating a 12-year-old female dog weighing 23 kg having breast cancer with 500 μCi of ^{131}I-labelled rMnSOD. Scintigraphic images of the abdomen (ventral view) obtained 3 and 24 hr after injection are shown in Figure 4. A mammary tumour, labelled "T," is clearly visible in the right lower quadrant in both early and late images. Non-specific retention could be detected in liver and stomach (LS) and in the urinary bladder in the 3-hr image and in the bowel in the 24-hr image. This shows that the protein could reach and localize at the tumour site with good selectivity even at an early stage after injection.

Immunocytochemical analyses of rMnSOD-treated MCF cells in the presence and absence of estradiol

Sensitive MCF-7 cells were then treated with a 1.5-μM concentration of rMnSOD in the presence or absence of a 10-nM solution of estradiol. MCF-7 cells treated only with DMEM supplemented with 10% FCS were used as a negative control. After 24 hr, light microscopy revealed that only the MCF-7 cells treated with an excess of estradiol and the negative control cells were viable. In contrast, the MCF-7 cells that received only rMnSOD had all died. These results were also confirmed by immunocytochemical analyses. After treatment with the solutions reported above, the cells were fixed and the presence of the rMnSOD inside the cells was determined by light microscopy following immunogold staining (Fig 5). In contrast to the untreated MCF-7 cells (A), MCF-7 cells treated with rMnSOD showed highly cytoplasmic immunoreactiv-

TABLE II – *IN VIVO* PHARMACOLOGY

Groups	Animals used (*N*)	Treatment	Daily dose (μg)	Total dose (μg)	Tumor size beginning	Tumor size end	Necrotic areas
1	2 × 6	None	None	None	1.5 cm	4.4 cm	Absent
2	12	rMnSOD	1	15	1.5 cm	3.2 cm	+
3	12	rMnSOD	2	30	1.5 cm	2.3 cm	++
4	12	rMnSOD	3	45	1.5 cm	1.9 cm	+++
5	12	rMnSOD	4	60	1.5 cm	1.3 cm	++++

Evaluation of tumour growth in nude mice bearing A2780 cell xenografts derived from a human ovarian adenocarcinoma and treated or not treated with intraperitoneal injection of increasing daily doses of rMnSOD. Control groups consisting of 6 animals each were untreated or received only PBS by injection.

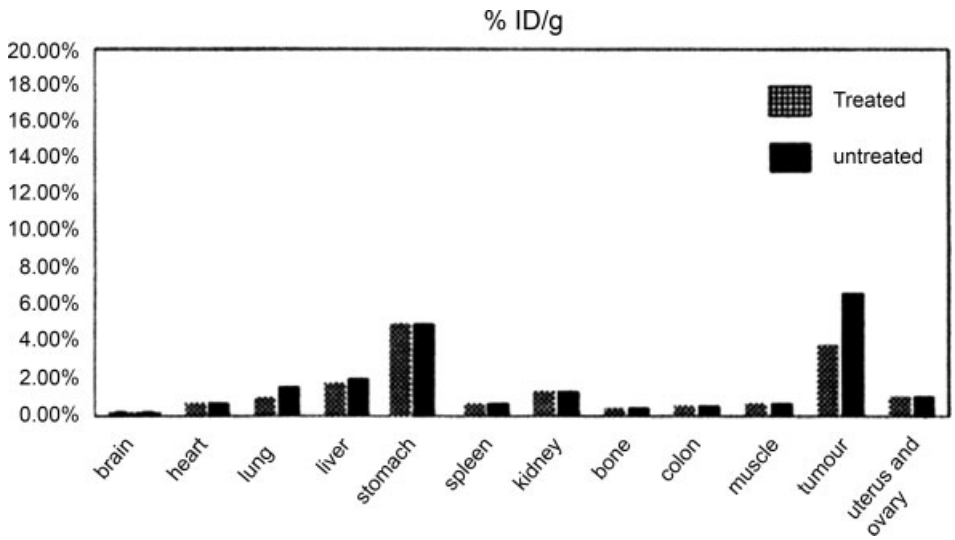

FIGURE 3 – *In vivo* uptake and biodistribution of rMnSOD. For the biodistribution study, nude mice bearing A2780 cell xenografts derived from a human ovarian adenocarcinoma were treated or not treated after the tumour was clinically evident, with a daily i.p. injection of 4 μg rMnSOD. After 15 days of treatment, an animal of each group (treated or not treated) was injected with ~5 μg of ^{125}I-labelled rMnSOD to study the biodistribution. The animals were killed 3 hr after the injection, dissected and organ counted in a single-well gamma counter. Dilutions of the injected compound were also counted to accurately determine the injected dose. The relative amount of radioactivity in the organs was calculated and expressed as percentage of the injected dose/gram tissue (%ID/g).

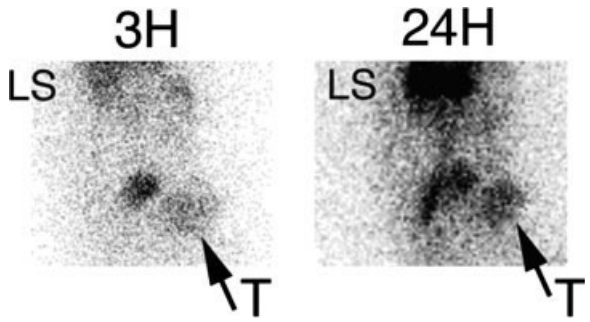

FIGURE 4 – Localization of ^{131}I-labelled rMnSOD in a dog with breast cancer. Scintigraphic images of the abdomen (ventral view) obtained 3 and 24 hr after injection of 500 μCi of ^{131}I-labelled rMnSOD in a 12-year-old female dog weighing 23 kg with breast cancer. A mammary tumour in the right lower quadrant is clearly visible in the early and late images (T). Non-specific retention is visible in liver and stomach (LS) and in the urinary bladder in the 3-hr image and bowel in the 24-hr image.

ity 1 hr after (B) and 2 hr after (B_1) the rMnSOD treatment, displaying a ghost-like feature indicating early necrosis and the cytoplasm filled with silver-enhanced immunogold particles. The same high immunoreactivity against the rMnSOD was detected outside the MCF-7 cells that were pre-incubated with an excess of estradiol. In this case the internalization of rMnSOD was impaired (C). The immunoreaction was found to be clearly negative when the MCF-7 cells were treated only with estradiol (C_1)

Cytotoxic effect of rMnSOD on MCF-7 cells pre-treated with estradiol

rMnSOD was added to the culture medium of sensitive MCF-7 cells at a final concentration of 1.5 μM, in the presence and absence of a 10-nM estradiol solution in DMEM supplemented with 10% FCS. The cytotoxic effect of rMnSOD was evaluated by measuring the LDH released by lysis from treated cells. In Figure 6 the amount of LDH released into the culture supernatant is expressed as a percentage of total LDH released from cell lysis following detergent treatment. Approximately 3% LDH was found in the medium of the control cultures not treated with rMnSOD.

In vitro *analysis with FITC-conjugated leader peptide*

The role that the non-excised 24-residue leader peptide might have in the unusual functions of the rMnSOD was investigated. A synthetic version of the leader peptide was then constructed and marked with fluorescein. A scrambled peptide with the same amino acid composition but a different sequence was also synthesized and used as control. Cultured MCF-7 cells were separately treated with the labelled leader peptide or the scrambled sequence for 1 hr at room temperature and then examined by confocal microscopy. Figure 7*a* shows the confocal laser scanning microscopy images of the equatorial sections of MCF-7 cells. Intense cytoplasmic fluorescence was clearly detected in the cells incubated with the leader peptide, demonstrating that the labelled peptide was able to permeate the cells under these conditions. No fluorescence was observed within the negative control cells treated with the scrambled peptide (Fig. 7*d*). In a different experiment, cultured MCF-7 cells were previously treated with a 1-μM oestrogen solution and then incubated with the labelled peptide. Confocal microscopy examination at the same focal plane of untreated cells (Fig. 7*b*) showed only a peripheral fluorescence outside the cells, confirming that peptide uptake was inhibited in the presence of oestrogen.

In vivo *analysis with ^{68}Ga-labelled DOTA-coupled leader peptide and PET imaging*

The synthetic leader sequence of rMnSOD was previously coupled with DOTA, labelled with ^{68}Ga and then injected into a dog bearing a spontaneous mammary tumour. Two hours after the injection the animal was examined by PET. Sagittal PET images (Fig. 8) showed a high concentration of the radiolabelled peptide in the tumour (T). The radiopharmaceutical was eliminated *via* the kidneys (K), where, along with the urinary bladder, the highest concentration of activity was seen in the images, ~10 times higher than in the tumour. In addition the liver (L) showed levels of uptake that were comparable to those observed in the tumours.

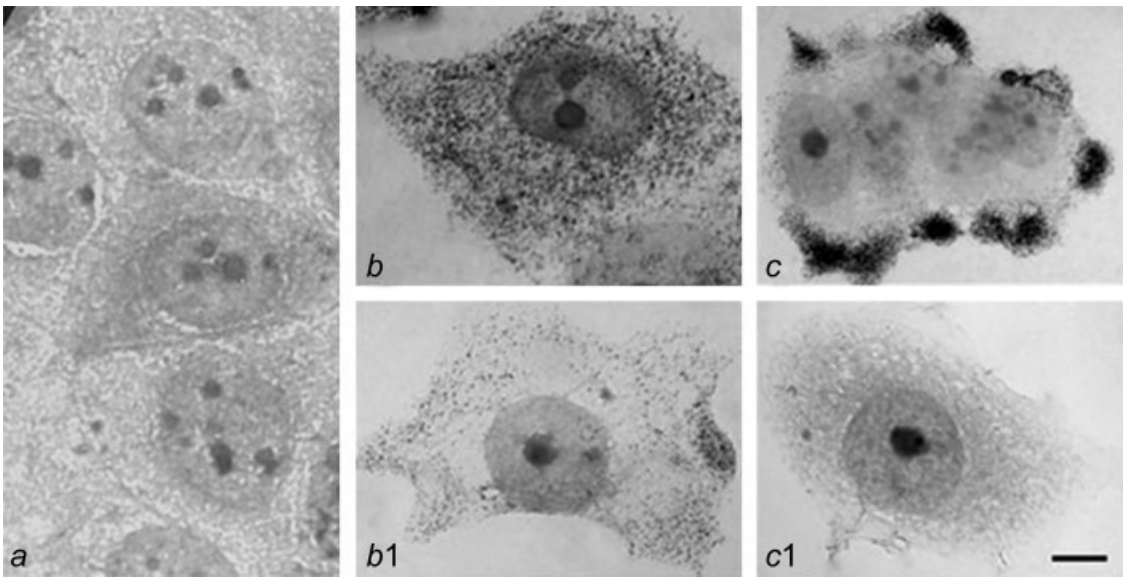

FIGURE 5 – Immunocytochemical analysis of rMnSOD-treated cells. Untreated MCF-7 cells (control, *a*) and MCF-7 cells treated with rMnSOD for 1 hr (*b*) and 2 hr (b_1), treated with rMnSOD and estradiol (*c*), and treated only with estradiol (c_1) were examined by light microscopy after rMnSOD labelling with immunogold and silver enhancer staining. Panel *a*: cluster of control MCF-7 cells showing the absence of immunostaining in the cytoplasm. Panel *b*: MCF-7 cells 1 hr after rMnSOD administration showing the cytoplasm filled with silver enhanced immunogold particles. Panel b_1: MCF-7 cells after 2 hr of rMnSOD treatment, displaying a ghost-like feature indicating early necrosis and the cytoplasm filled with silver enhanced immunogold particles. Panel *c*: MCF-7 cell clusters treated with rMnSOD (1.5-μM) and estradiol showing a large amount of silver-enhanced immunogold particles located in the medium outside the cell. Panel c_1: cultured MCF-7 cells treated only with estradiol showing the absence of immunostaining in the cytoplasm. Scale bar (in c_1) = 7 μm.

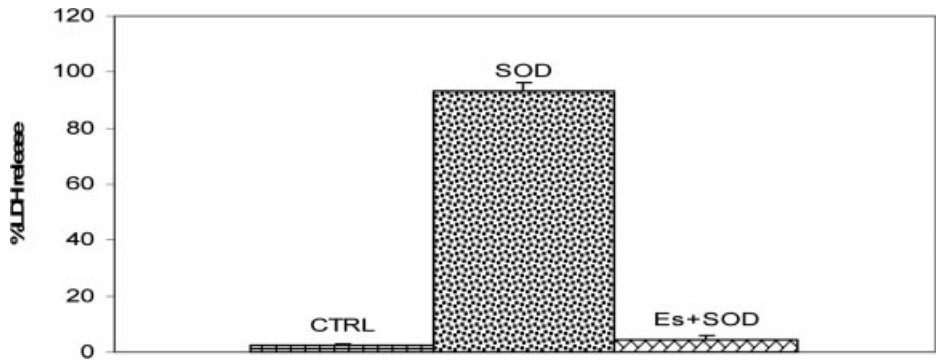

FIGURE 6 – Cytotoxic effect of rMnSOD on MCF-7cells pretreated with estradiol. The cytotoxic effect of rMnSOD on MCF7 cells in the presence and absence of estradiol was evaluated by measuring the amount of LDH released in the culture supernatant. rMnSOD-released LDH is expressed as a percentage of total LDH measured from cells after lysis following detergent treatment.

PCR analyses

The possible pro-apoptotic effects of rMnSOD on tumour cells were investigated by PCR expression analysis of the pro-apoptotic *Bax* gene and the anti-apoptotic *Bcl2* gene. Three samples of MCF7 breast cancer cells were cultured in DMEM + 10% FCS in the presence of 1.5-μM rMnSOD; 3 control samples of MCF-7 cells were maintained under identical culture conditions but in the absence of rMnSOD. The total RNA extracted from the 6 cell samples was reverse-transcribed and both *Bax* and *Bcl2* cDNAs were amplified by PCR analysis. Figure 9 shows the amplified fragments of both *Bax* (460 bp) and *Bcl2* cDNAs (205 bp) in the different experimental conditions. A strong *Bax* transcript band was clearly detected in all the samples of MCF-7 cells cultured in the presence of rMnSOD (Panel *a*, lanes *a*, *b* and *c*) that was absent in the controls. In contrast, *Bcl2* gene expression could only be detected in MCF7 cells in the absence of rMnSOD (Panel *b*, lanes *d*, *e* and *f*) whereas its expression was totally impaired by rMnSOD treatment. The actin transcript band (500 bp) unaffected by rMnSOD treatment was used to control for the quantity of cDNA (Panel *c*).

Discussion

This article reports the biochemical, biophysical and functional characterization of rMnSOD, a recombinant manganese superoxide dismutase produced and actively secreted by a human liposarcoma cell line cultivated in a chemically defined medium into which the protein has been released. Both the original LSA-type MnSOD and the recombinant enzyme were previously found to exhibit oncosuppressive activity *in vitro* and *in vivo*.[10] Wild-type MnSOD is normally located within the mitochondrial matrix following cleavage of the leader sequence and is not endowed with any oncosuppressive activity.

The active secretion of the LSA-type MnSOD by LSA cells and its ability to act as an oncosuppressor suggested that certain struc-

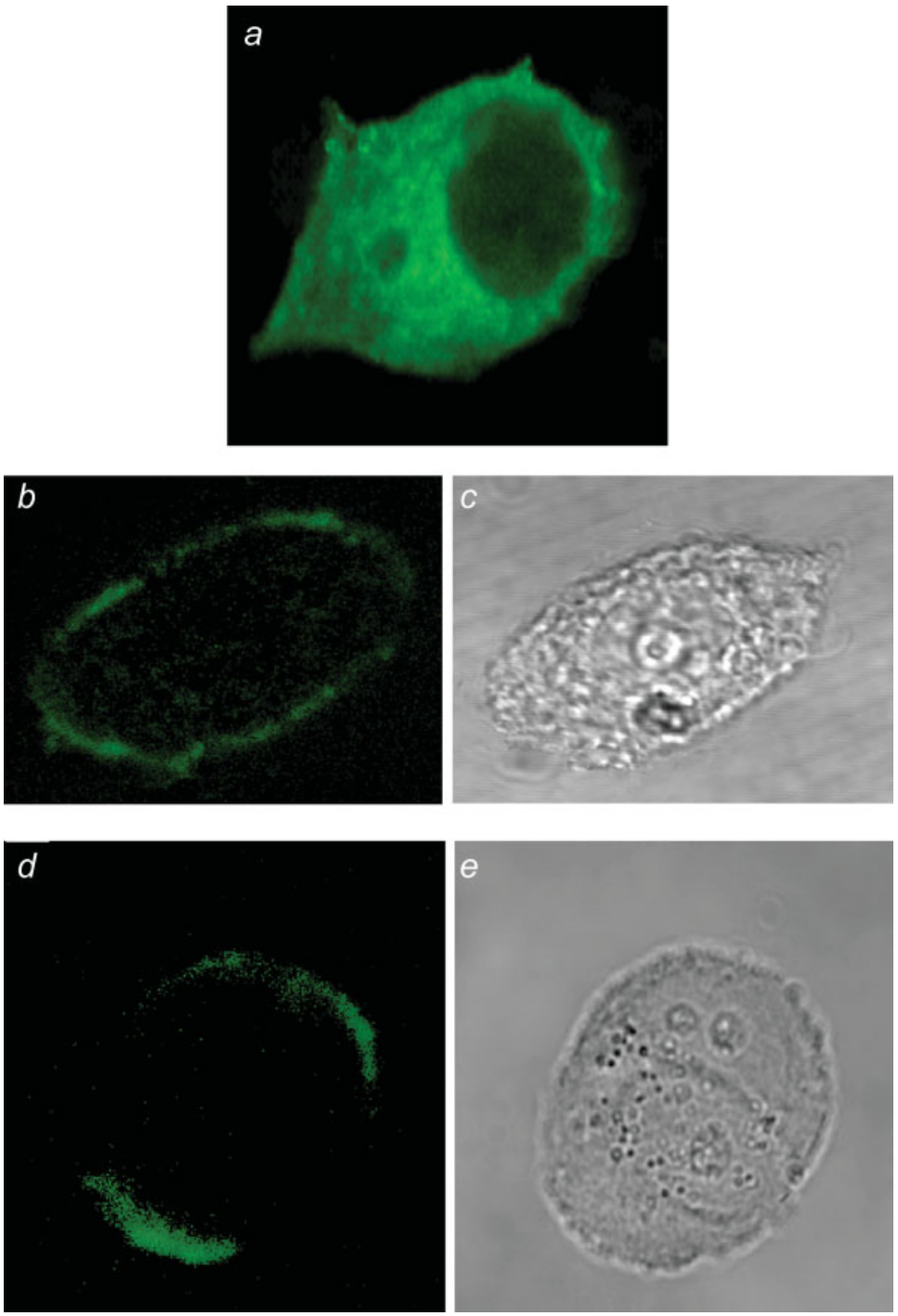

FIGURE 7 – Fluorescence confocal microscopic analysis of rMnSOD leader peptide distribution in treated MCF-7 cells. Equatorial sections of FITC-labelled MCF-7 cells are shown. (*a*) MCF-7 cell not pre-treated with oestrogen. FITC-labelled peptide permeated the cell and filled the entire cytoplasm 1 hr after treatment. (*b*) MCF-7 cell pre-treated with oestrogen: FITC-labelled peptide remains outside the cell (phase contrast image in panel (*c*). (*d*) Control MCF-7 cell treated with FITC-labelled scrambled peptide and (phase contrast image in Panel *e*).

tural modifications might account for these unusual properties. A detailed structural characterization of the recombinant product both at the protein and cDNA level clearly demonstrated that rMnSOD retains the leader sequence at the N-terminus and contains an additional pentapeptide at the C-terminus. Since the presence of the 5 C-terminal residues was due to a single point mutation during genetic manipulation, the principal difference between the wild-type MnSOD and rMnSOD was the persistence of the leader peptide in the recombinant form. The structural analysis was also extended to the LSA-type MnSOD, the isoform secreted from LSA cells endowed with anti-tumoural activity,[10] confirming the presence of the leader peptide at the N-terminus and ruling out the occurrence of an additional pentapeptide at the C-terminus, as expected. Because the oncotoxic activity is present both in the original LSA-type MnSOD and in rMnSOD, the presence of the leader peptide was strongly suspected, not only considering the

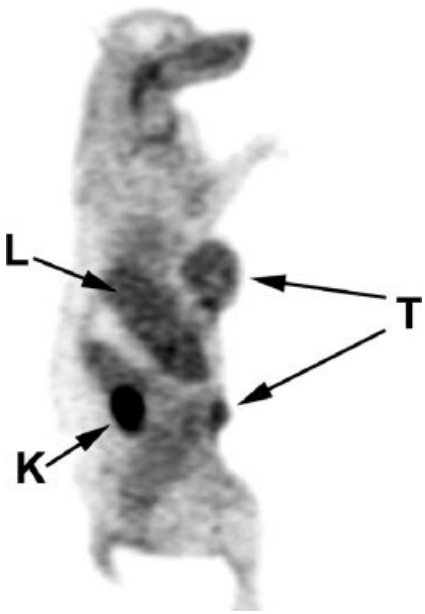

FIGURE 8 – PET analysis of ^{68}Ga-labelled DOTA-coupled peptide in a treated tumour-bearing dog. The sagittal view shows a high concentration of the radiolabelled peptide in the tumour (T). The radiopharmaceutical was eliminated through the kidneys (K) which, along with the urinary bladder, showed the highest signal in the images, ~10 times higher than in the tumour. The liver (L) showed levels of uptake that were comparable to those observed in the tumour.

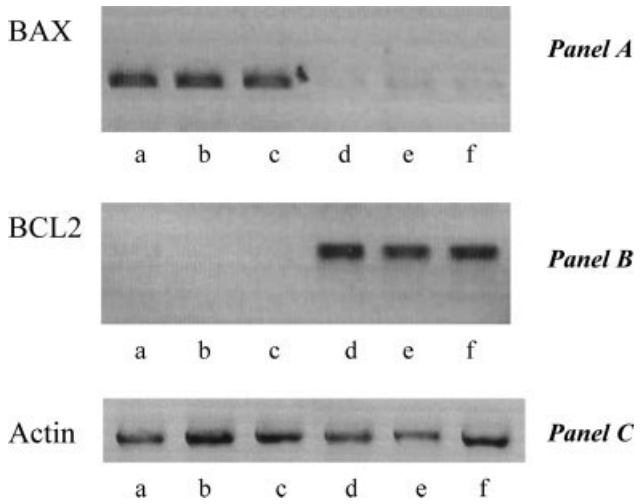

FIGURE 9 – PCR analysis of apoptotic resgulator expression in rMnSOD-treated cells. Amplification of Bax and Bcl2 cDNAs from MCF-7 cells treated or not treated with rMnSOD. Both samples were prepared in triplicate. Panel *a*, lanes *a*, *b* and *c* show the amplified Bax cDNA fragment (460 bp) from MCF-7 cells treated with rMnSOD. Control lanes are *d*, *e* and *f*. Panel *b*, lanes *a*, *b* and *c* show the absence of amplified Bcl2 cDNA fragments (205 bp) from MCF-7 cells treated with rMnSOD. Control lanes are *d*, *e* and *f*. Panel *c* shows the actin PCR product (500 bp) as control of cDNA quantity.

unusual secretion of the molecule from LSA cells as previously reported[9] but also because of the specific and selective uptake by tumour cells.

rMnSOD is enzymatically active even in the presence of the leader sequence, whereas the wild-type enzyme requires that the leader peptide is released in order to be transformed in the mature, active form.[16] Characterization of the secondary structure and the stability of the recombinant protein rMnSOD was then investigated. The far-UV CD spectra of rMnSOD indicated that the secondary structure of the protein is similar to that of human MnSOD as shown by its crystallographic structure.[21] Thermal unfolding of rMnSOD, also monitored by CD spectra, was followed by an irreversible aggregation of the unfolded molecule. The unfolding temperature (59°C) is about 30° lower than that of native human MnSOD. On the basis of the crystal structure of human MnSOD, the additional peptide fragments present at the N-terminal of rMnSOD should not interfere with the dimer and tetramer association, as they are far away from the subunit interface. The decrease in the thermal stability of rMnSOD with respect to the wild-type protein suggests that the subunit fold is destabilized, partly due to the presence of the leader peptide at the N-terminus and partly to the partial occupancy of the metal ion-binding sites.[23] The internalized rMnSOD may increase the level of oxidants (hydrogen peroxide and hydroxyl radicals), which are known to mediate cell killing.[24–26] The addition of rMnSOD to MCF-7 cells generated increasing amounts of hydrogen peroxide and total SODs inside the tumour cells. In contrast, the cell-associated H_2O_2 concentrations in resistant MRC-5 cells remained constant, regardless of whether cultures had been treated with rMnSOD. Treatment of MCF-7 cells with a commercially available SOD preparation (which essentially consists of a mixture of Zn/Cu-SOD and MnSOD) as control did not provide the same results (data not shown). These results confirmed that Zn/Cu-SOD is structurally and functionally different from rMnSOD.[27,28] Several reports suggested that MnSOD may have tumour suppressor functions but its role in cancer development remained elusive although it has long been known that reactive oxygen species (ROS) are increased in cancer cells. Indeed, most cells have abundant Cu/Zn-SOD and glutathione peroxidase (Gpx) to dismutate ROS into molecular oxygen and water, making an anti-cancer mechanism of rMnSOD questionable. Moreover, previous studies showed increased levels of both Zn/Cu-SOD and MnSOD in cancer cells of various tissue origins whereas high levels of MnSOD expression[29–31] have been detected in various primary human cancer tissues and in blood samples from patients with various types of leukaemia.[32] However, as MnSOD levels seem to decrease in certain cancer cells and forced expression of MnSOD appears to suppress malignant phenotypes in certain experimental models, only MnSOD, and not Zn/Cu-SOD, was considered as a tumour suppressor protein.[33] This was supported by the finding that suppression of MnSOD expression by siRNA promotes O_2^- accumulation and also cell proliferation *in vitro* and tumour growth *in vivo*.[34]

In an attempt to define the mechanism underlying the cytotoxic effects of rMnSOD, the expression levels of 2 apoptotic genes were examined by PCR. A strong upregulation of pro-apoptotic Bax gene expression was clearly observed in tumour cells in the presence of rMnSOD as compared to the control, suggesting that treatment with the recombinant protein might induce the apoptotic cascade in tumour cells. The possible involvement of an apoptotic mechanism was confirmed by the strong inhibition of anti-apoptotic Bcl2 gene expression detected in tumour cells in the presence of rMnSOD. Although more data are needed to support these conclusions, the induction of an apoptotic program might explain the specific and selective cytotoxicity exerted by rMnSOD on cancer cells at the molecular level.

The *in vivo* analysis demonstrated a dose-dependent cytotoxic effect of rMnSOD. Biodistribution studies of rMnSOD performed to investigate its specific uptake and catabolic excretion provided information for a more rational pharmacological use of the molecule. These studies aimed to evaluate the *in vivo* anti-tumoural activity of rMnSOD and to investigate which organs would preferentially take up the molecule and, hence, to define the toxicity risk of each organ related to the administration of the protein. The ^{125}I-labelled rMnSOD was injected into nude mice bearing ovarian carcinomas and the amount of radioactivity incorporated was evaluated. The tumours in nude mice showed radioactivity levels 3 or

4 times higher than those in normal organs, demonstrating the specificity of the molecule to reach the tumour in the body.

The role the leader peptide has in these unusual oncotoxic functions of rMnSOD was investigated by using synthetically constructed fragments. The fluorescein-labelled leader peptide was indeed able to permeate MCF-7 cells and exhibited a diffuse cytosolic distribution of fluorescence. Moreover, the uptake of the leader peptide was clearly inhibited when the target cells were previously treated with an excess of oestrogen. A scrambled FITC-labelled peptide used as control could not permeate the tumour cells. The function of the leader peptide was also assessed by *in vivo* experiments. One hour after injecting the ^{68}Ga-labelled synthetic peptide, PET images of a dog suffering from spontaneous breast cancer showed that the peptide was localized in all the lesions of the body, both primary and metastatic. Both of these analyses confirmed that the leader peptide might function as a molecular carrier, suggesting that the peptide moiety might be used to transport several drugs and molecules into the tumour cells. Moreover, the synthetic ^{68}Ga-labelled peptide might also have a role as a diagnostic and prognostic marker in conjunction with PET scans and rMnSOD treatment.

Previous observations suggested that rMnSOD exerts its cytotoxic activity only on tumour cells expressing oestrogen receptors (ER^+). Although the molecular mechanism underlying rMnSOD incorporation into tumour cells still needs to be fully clarified, the results reported in this article clearly demonstrate that the uptake of both rMnSOD and the leader peptide is inhibited by the presence of an excess of oestrogen. A possible explanation might be the sequestration of the cell surface forms of ER as a result of the oestrogen excess, and thus impairing rMnSOD uptake. Alternatively, the estradiol might affect the expression of other receptors responsible for rMnSOD uptake. In any case, although these findings restrict the range of activity of rMnSOD to ER^+ tumour cells, the recombinant molecule appears to be effective against ER^+ tumours.

The specific and selective uptake of rMnSOD into tumour cells was also confirmed by injecting ^{131}I-labelled rMnSOD into a female dog affected by spontaneous breast cancer. These *in vivo* results are in keeping with our previous pharmacological *in vitro* observations[10] and might have specific implications. If the most important feature required for a cytostatic drug is the ability to reach the tumour, then we could foresee a broad usage of rMnSOD in cancer treatment. Besides functioning as an anti-tumoural drug, which in itself could be considered a satisfactory result, the recombinant protein and/or its leader sequence might also be used both as a specific marker for image analysis and as a radiopharmaceutical vehicle. Indeed, the rMnSOD molecule can be labelled with a beta or gamma emitter isotope and injected into an organism in which the presence of a tumour is suspected. The scintigraphic or PET examination of the organism will reveal the presence of a tumour as a result of the specific and selective uptake of the labelled protein by the cancer cells. Moreover, a possible simultaneous therapeutic effect might be exerted by both the oncotoxic property of the protein *per se* and the radioactive (gamma and/or beta) emission of the protein-bound tracer. These possibilities underline the diagnostic and therapeutic value of radiolabelled rMnSOD as an anticancer agent. Experiments are in progress in our laboratory to use the labelled rMnSOD as an effective means to combat and hopefully cure cancer, especially if used in combination with more conventional treatments (surgery, chemotherapy and radiotherapy).

In conclusion, the present study gives strong evidence that rMnSOD and its leader sequence deserve to be considered for the treatment and diagnosis of cancer. In addition to the potent oncotoxic and oncosuppressive effects supported by both *in vitro* and *in vivo* experiments, this protein is the only human MnSOD available and can be produced in an active recombinant form and easily administered to patients with tumours. Although the structural and functional parameters of the molecule have been extensively characterized, the tumour specificity still needs to be clarified in more detail, in particular regarding its correlation with the persistence of the leader sequence and the involvement of oestrogen receptors. Work is in progress to clarify the role of the leader sequence, especially to determine whether it is the key through which the molecule is able to be taken up by ER^+ cancer cells. If this is true, then the intriguing possibility exists to define and use only the recognition peptide to deliver any kind of cytotoxic agent to the tumour cells, ensuring and amplifying their cytotoxic effects, or to use it as a carrier for gene therapy.

Acknowledgements

The authors are deeply indebted to Dr. Giovanni Paganelli (European Institute of Oncology-IEO) for critical evaluation of this study.

References

1. Bishop JM. The molecular genetics of cancer. Science 1987;235:305–11.
2. Rabbitts TH. Chromosomal translocations in human cancer. Nature 1994;372:143–9.
3. Mitelman F, Mertens F, Johansson B. A breakpoint map of recurrent chromosomal rearrangements in human neoplasia. Nat Genet 1997;15:417–74.
4. Doll R, Peto R. The causes of cancer: quantitative estimates of avoidable risks of cancer in the United States today. J Natl Cancer Inst 1981;66:1191–308.
5. Sun J, Hemler ME. Regulation of MMP-1 and MMP-2 production through CD147/extracellular matrix metalloproteinase inducer interactions. Cancer Res 2001;61:2276–81.
6. Folkman J. Tumor angiogenesis: a possible control point in tumor growth. Ann Intern Med 1975;82:96–100.
7. Konopka TE, Barker JE, Bamford TL, Guida E, Anderson RL, Stewart AG. Nitric oxide synthase II gene disruption: implications for tumor growth and vascular endothelial growth factor production. Cancer Res 2001;61:3182–7.
8. Arbiser JL, Petros J, Klafter R, Govindajaran B, McLaughlin ER, Brown LF, Cohen C, Moses M, Kilroy S, Arnold RS, Lambeth JD. Reactive oxygen generated by Nox1 trigger the angiogenic switch. Proc Natl Acad Sci USA 2002;99:715–20.
9. Mancini A, Garbi C, D'Armiento FP, Borrelli A, Ambesi-Impiombato FS. Culture and cloning of an adipocytes cell line froma human liposarcoma. Bollettino Istituto dei Tumori di Napoli 1991;38:43–49.
10. Mancini A, Borrelli A, Schiattarella A, Fasano S, Occhiello A, Pica A, Sehr P, Tommasino M, Nüesch JP, Rommelaere J. Tumor suppressive activity of a variant isoform of manganese superoxide dismutase released by a human liposarcoma cell line. Int J Cancer 2006;119:932–43.
11. McCord JM, Fridovich I. Superoxide dismutase. An enzymic function for erythrocuprein (hemocuprein). J Biol Chem 1969;244:6049–55.
12. Folz RJ, Guan J, Seldin MF, Oury TD, Enghild JJ, Crapo JD. Mouse extracellular superoxide dismutase: primary structure, tissue-specific gene expression, chromosomal localization, and lung in situ hybridization. Am J Respir Cell Mol Biol 1997;17:393–403.
13. Ookawara T, Kizaki T, Yakayama E, Imazeki N, Matsubara O, Ikeda Y, Suzuki K, Li Ji L, Tadakuma T, Taniguchi N, Ohno H. Nuclear translocation of extracellular superoxide dismutase. Biochem Biophys Res Comm 2002;296:54–61.
14. Borgstahl GE, Parge HE, Hickey MJ, Beyer WF, Jr, Hallewell RA, Tainer JA. The structure of human mitochondrial manganese superoxide dismutase reveals a novel tetrameric interface of two 4-helix bundles. Cell 1992;71:107–18.
15. Davis CA, Hearn AS, Fletcher B, Bickford J, Garcia JE, Leveque V, Melendez JA, Silverman DN, Zucali J, Agarwal A, Nick HS. Potent anti-tumor effects of an active site mutant of human manganese-superoxide dismutase. Evolutionary conservation of product inhibition. J Biol Chem 2004;279:12769–76.
16. Wispe JR, Clark JC, Burhans MS, Kropp KE, Korfhagen TR, Whitsett JA. Synthesis and processing of the precursor for human manganosuperoxide dismutase. Biochim Biophys Acta 1989;994:30–6.
17. Corbau R, Salomon N, Rommeleare J, Nuesch JP. Phosphorylation of the viral non structural protein NS1 during MVMp infection of A9 cells. Virology 1999;259:402–15.

18. Holgate CS, Jackson P, Cowen PN, Bird CC. Immunogold-silver staining: new method of immunostaining with enhanced sensitivity. J Histochem Cytochem 1983;31:938–44.
19. Stewart JM, Young JD. Solid phase peptide synthesis. Rockford, IL: Pierce Chemical, 1984.
20. Matthias M, Hendrickson RC, Pandey RC. Analysis of proteins and proteosomes by mass spectrometry. Annu Rev Biochem 2001;70: 437–73.
21. Wagner UG, Pattridge KA, Ludwig ML, Stallings WC, Werber MM, Oefner C, Frolow F, Sussman JL. Comparison of the crystal structures of genetically engineered human manganese superoxide dismutase and manganese superoxide dismutase from Thermus thermophilus: differences in dimer-dimer interaction. Protein Sci 1993;2:814–25.
22. Mizuno K, Whittaker MM, Bächinger HP, Whittaker JW. Calorimetric studies on the tight binding metal interactions of Escherichia coli manganese superoxide dismutase. J Biol Chem 2004;279:27339–44.
23. Hsieh Y, Guan Y, Tu C, Bratt PJ, Angerhofer A, Lepock JR, Hickey MJ, Tainer JA, Nick HS, Silverman DN. Probing the active site of human manganese superoxide dismutase: the role of glutamine 143. Biochemistry 1998;37:4731–9.
24. Mashiba H, Matsunaga K. Device for intracellular increase of oxygen free radicals and inhibition of MethA tumour cell proliferation: in vitro and in vivo studies. Int J Tissue React 1988;10:273–80.
25. Schimmel M, Bauer G. Proapoptotic and redox state-related signaling of reactive oxygen species generated by transformed fibroblasts. Oncogene 2002;21:5886–96.
26. Mainous AG, III, Wells BJ, Koopman RJ, Everett CJ, Gill JM. Iron, lipids, and risk of cancer in the Framingham Offspring cohort Am J Epidemiol 2005;161:1115–22.
27. Wheeler MD, Smutney OM, Samulski RJ. Secretion of extracellular superoxide dismutase from muscle transduced with recombinant adenovirus inhibits the growth of B16 melanomas in mice. Mol Cancer Res 2003;1:871–81.
28. Mondola P, Annella T, Santillo M, Santangelo F, Mondola P, Annella T, Santillo M, Santangelo F. Evidence for secretion of cytosolic CuZn superoxide dismutase by Hep G2 cells and human fibroblasts. Int J Biochem Cell Biol 1996;28:677–81.
29. Janssen AM, Bosman CB, Kruidenier L, Griffioen G, Lamers CB, van Krieken JH, van de Velde CJ, Verspaget HW. Superoxide dismutases in the human colorectal cancer sequence. J Cancer Res Clin Oncol 1999;125:327–35.
30. Janssen AM, Bosman CB, van Duijn W, Oostendorp-van de Ruit MM, Kubben FJ, Griffioen G, Lamers CB, van Krieken JH, van de Velde CJ, Verspaget HW. Superoxide dismutases in gastric and esophageal cancer and the prognostic impact in gastric cancer. Clin Cancer Res 2000;6:3183–92.
31. Punnonen K, Ahotupa M, Asaishi K, Hyöty M, Kudo R, Punnonen R. Antioxidant enzyme activities and oxidative stress in human breast cancer. J Cancer Res Clin Oncol 1994;120:374–7.
32. Nishiura T, Suzuki K, Kawaguchi T, Nakao H, Kawamura N, Taniguchi M, Kanayama Y, Yonezawa T, Lizuka S, Taniguchi N. Elevated serum manganese superoxide dismutase in acute leukemias. Cancer Lett 1992;62:211–5.
33. Church SL, Grant JW, Ridnour RA, Oberlay LW, Swanson PE, Meltzer PS, Trent JM. Increased manganese superoxide dismutase expression suppresses the malignant phenotype of human melanoma cells. Proc Natl Acad Sci USA 1993;90:3113–17.
34. Hu Y, Rosen DG, Zhou Y, Feng L, Yang G, Liu J, Huang P. Mitochondrial manganese-superoxide dismutase expression in ovarian cancer: role in cell proliferation and response to oxidative stress. J Biol Chem 2005;280:39485–92.